Biochars intended for water filtration: A comparative study with activated carbons of their physicochemical properties and removal efficiency towards neutral and anionic organic pollutants

Biochars intended for water filtration: a comparative study with activated carbons of their physicochemical properties and removal efficiency towards neutral and anionic organic pollutants

Michele Castiglioni[a], Luca Rivoira[a], Irene Ingrando[a], Lorenza Meucci[b], Rita Binetti[b], Martino Fungi[b], Ayoub El-Ghadraoui[c], Zaineb Bakari[c,d], Massimo Del Bubba[c], Maria Concetta Bruzzoniti[a*]

[a] Department of Chemistry, University of Turin, Via P. Giuria 5, 10125 Turin, Italy

[b] SMAT S.p.A., Research Centre, C.so Unità d'Italia 235/3, Turin, Italy

[c] Department of Chemistry "Ugo Schiff", University of Florence, Via della Lastruccia 3, 50019 Sesto Fiorentino, Italy

[d] National Engineering School of Sfax, Route de la Soukra km 4, 3038 Sfax, Tunisia

*Corresponding Author, contact information

Prof. Maria Concetta Bruzzoniti

Department of Chemistry, University of Turin, Via P. Giuria 5, 10125 Turin (Italy)

Email: mariaconcetta.bruzzoniti@unito.it

Phone: +390116705277

Fax: +390112365277

Orcid: 0000-0002-9144-9254

Abstract

Seven biochars (BCs) obtained from pyrolysis or gasification of different vegetal feedstocks were thoroughly characterized in comparison with three commercial activated carbons (ACs) routinely used in drinking water treatment plants. BCs and ACs characterization included the determinations of ash, iodine and methylene blue adsorption indexes, and the release of metals and polycyclic aromatic hydrocarbons, which were performed according to international standards applied for adsorption media to be used in drinking waters. Total specific surface area, micropore and mesopore specific surface area, pH of the point of zero charge, and the release of polychlorinated biphenyls were also determined in all chars. Principal component analysis and cluster analysis were performed in order to summarize the complex set of information deriving from the aforementioned characterizations, highlighting the BC most similar (BC6 from high temperature gasification of woody biomass) and most different (BC7 from low-temperature pyrolysis of corn cob) from ACs. These BCs were studied for their adsorption in ultrapure water towards diiodoacetic acid (an emergent disinfection by-product), benzene, and 1.2-dichlorobenzene, in comparison with ACs, and results obtained were fitted by linearized Freundlich equation. Overall, BC6 showed higher sorption performances compared to BC7, even though both BCs were less performing sorbents than ACs. However, the sorption properties of BCs were maintained also in real water samples collected from drinking water treatment plants.

Keywords: pyrolysis, gasification, filtration media, PAH and PCB release, metal release, drinking water plant

1 Introduction

Pollution by anthropic activities still affects the quality of water resources. According to the European Water Framework Directive (2000/60/EU), waters must achieve good ecological and chemical status, to protect human health, water supply, natural ecosystems and biodiversity (European Commission, 2010).

The accomplishment of the environmental objectives set by the European policies can be achieved through proper integrated water management policies and technological approaches, which must be sustainable from both environmental and economic points of view. Within this framework, water treatments play significant and crucial roles in the supply of safe waters intended for human consumption.

Adsorption is an effective and economically feasible approach routinely integrated in drinking water production (Ali and Gupta, 2006) for the removal of micropollutants occurring *per se* in raw waters and/or as a result of disinfection processes, thereby eliminating the toxicity induced by these molecules in treated water (Han and Zhang, 2018; Han et al., 2021). Within this context, adsorption is generally based on the use of activated carbon (Jiang et al., 2017; Perrich, 2018; Jiang et al., 2020), even though innovative sorbents, such as mesoporous silica (Kyzas and Matis, 2015; Rivoira et al., 2016) or other waste-derived ceramic materials (Jana et al., 2016; Bruzzoniti et al., 2018) have been proposed as alternative adsorption media. Low-cost materials like biochar (BC) have recently received attention for their physicochemical characteristics including the porous structure, which is similar to that of activated carbons. Biochar is the solid by-product of the thermal conversion of a wide range of feedstocks, such as agricultural wastes (Ali and Gupta, 2006; Colantoni et al., 2016), wood residues (Wang et al., 2013), manure (Cao and Harris, 2010), and sludge (Méndez et al., 2017). Due to its properties, biochar has found application as animal feed additives (McHenry, 2010) and soil amenders (Singh et al., 2010), as well as for the adsorption of micropollutants from aqueous matrices (Palansooriya et al., 2020).

Internationally recognized standards detailing the physicochemical characteristics of biochars to be used for agricultural applications have been recently released (European Biochar Foundation (EBC)). Similar standards have not yet been established on the characteristics required for biochars to be used in water purification. However, international standards are available that require compliance with specific limits for certain physical and chemical parameters in adsorbent materials (Comite Europeen de Normalisation (CEN), 2004), and particularly in activated carbons (Comite Europeen de Normalisation (CEN), 2009), used for the treatment of drinking water.

In the last years, biochars obtained from a very wide range of experimental conditions (e.g. feedstock, thermo-chemical process and pretreatment of biomass and/or post-treatment of biochar) were investigated as sorbent media for water purification issues, highlighting their promising adsorption properties towards a large variety of organic and inorganic contaminants (Gwenzi et al., 2017; Wang et al., 2020). However, it should be emphasized that, with few exceptions (Del Bubba et al., 2020) it is not verified whether the biochars prepared in the various experimental conditions comply with the requirements set out in the aforementioned standards, relating to the absorbent materials intended to be used for the filtration of drinking water. Moreover, in most cases, ultrapure water is used to investigate sorption capabilities of biochars, whilst it would be advisable to perform these studies using real aqueous matrixes. Last but not least, except in rare cases (Del Bubba et al., 2020), no comparison has been made with the adsorption capacity of standard activated carbons (ACs). All these aspects represent obvious limitations in the reliable evaluation of the applicability of biochars for water treatment (Castiglioni et al., 2021).

Based on the considerations mentioned above, the aim of this research was to investigate the physicochemical properties, the regulated leachable substances, and the removal performances of seven biochars (commercially available or synthesized for the purpose), obtained from pyrolysis or gasification of vegetal biomass, in comparison with three commercially available vegetal ACs used in an Italian drinking water facility, at different age of operation. Data obtained were chemometrically treated through principal component analysis, allowing for selecting the most promising biochars to

be further investigated by adsorption tests. In a first phase of this study, adsorption capabilities were tested in ultrapure water, whereas afterwards the sorption capacity was evaluated on a restricted group of biochars in water samples collected at intermediate treatment stages of a potabilization plant. In all cases ACs were also tested as reference comparative materials.

Diiodoacetic acid (DIAA), benzene, and 1,2 dichlorobenzene, were selected as model pollutants commonly monitored in drinking water facilities. Specifically, DIAA is a model emerging disinfection by-product (Bruzzoniti et al., 2019b) never investigated before for its sorption by biochars. Moreover, 1,2 dichlorobenzene can also originate from disinfection treatments during the potabilization process (Lahaniatis et al., 1994; Hou et al., 2012) and its monitoring in tap water is recommended by the World Health Organization guidelines (taste threshold value 1 µg L^{-1}) (World Health Organization, 2017), while benzene is regulated by the Directive 2020/2184 regarding the quality of water intended for human consumption (1 µg L^{-1}). It should also be noted that benzene and 1,2 dichlorobenzene are volatile organic carbons (VOCs) still detected in some industrial districts (Martínez et al., 2002) and are therefore also important from the wastewater treatment viewpoint.

2 Materials and methods

2.1 Reagents

For the determination of adsorption indexes, the following reagents, supplied by Merck (Kenilworth, NJ, USA), were used: iodine solution (0.1 N), sodium thiosulfate solution (0.1 N), zinc iodide starch solution, hydrochloric acid (37%), potassium hexacyanoferrate (>99%), methylene blue, anhydrous acetic acid (>99.8%). Ammonia solution (28%), dichloromethane and 2-propanol were from VWR International (Radnor, PA, USA). For the evaluation of extractable metals, an ICP multi-element standard solution IX (100 mg L^{-1} of As, Be, Cd, Cr (VI), Ni, Pb, Se, Tl) from Merck was used.

For the determination of extractable polycyclic aromatic hydrocarbons (PAHs), the 16 compounds listed by EPA were purchased from Sigma Aldrich (Darmstadt, Germany). For the analysis of extractable polychlorinated biphenyls (PCBs), the compounds were purchased from LGC Standards (Milan, Italy). They were non dioxin-like PCBs: 3,3'-dichlorobiphenyl (PCB 11), 4,4'-

dichlorobiphenyl (PCB 15), 2,4,4'-trichlorobiphenyl (PCB 28), 2,2',5,5'-tetrachlorobiphenyl (PCB 52), 2,2',4,5,5'-pentachlorobiphenyl (PCB 101), 2,2',3,4,4',5-hexachlorobiphenyl (PCB 138), 2,2',4,4',5,5'-hexachlorobiphenyl (PCB 153), 3,3',4,4',5,5'-hexachlorobiphenyl (PCB 169), 2,2',3,4,4',5,5'-heptachlorobiphenyl (PCB 180), 2,3,3',4,4',5,5'-heptachlorobiphenyl (PCB 189); and dioxin-like PCBs: 3,4,4',5-tetrachlorobiphenyl (PCB 81), 2,3',4,4',5-pentachlorobiphenyl (PCB 118), 2',3,4,4',5-pentachlorobiphenyl (PCB 123), 2,3',4,4',5,5'-hexachlorobiphenyl (PCB 167).

Labelled isotope compounds for PCBs (2 mg L^{-1}) and for PAHs (5 mg L^{-1}), Wellington Laboratories (Ontario, Canada), were used as internal and surrogate standards in order to obtain calibration curves and extraction recoveries, respectively. The ^{13}C surrogate solutions of PAHs contained: [$^{13}C_6$]benzo(a)anthracene [$^{13}C_6$-BaA], [$^{13}C_6$]chrysene [$^{13}C_6$-Chr], [$^{13}C_6$]benzo(b)fluoranthene [$^{13}C_6$-BbFl], [$^{13}C_6$]benzo(k)fluoranthene [$^{13}C_6$-BkFl], [$^{13}C_4$]benzo(a)pyrene [$^{13}C_4$-BaP], [$^{13}C_6$]indeno(1,2,3-cd)pyrene [$^{13}C_4$-Ind], [$^{13}C_6$]dibenzo(a,h)anthracene [$^{13}C_6$-DBA], and [$^{13}C_{12}$]benzo(g,h,i)perylene [$^{13}C_{12}$-BP]. The ^{13}C surrogate solution of PCBs contained: $^{13}C_{12}$-PCB28, $^{13}C_{12}$-PCB52, $^{13}C_{12}$-PCB118, $^{13}C_{12}$-PCB153, and $^{13}C_{12}$-PCB180.

Volatile organic compounds, namely benzene (100 µg L^{-1} in methanol), and 1,2-dichlorobenzene (100 µg L^{-1} in methanol), were purchased from Ultra Scientific Italia (Bologna, Italy). DIAA was supplied by Chemical Research (Rome, Italy). Ultrapure water was obtained by an EMD Millipore Milli-Q Direct Water Purification System (Millipore, Bedford, MA, USA).

2.2 Biochar and activated carbon samples

The seven BCs considered in this study were donated for the purpose by different companies, which produce the materials for commercial scopes or for their internal use through well-established procedures. The three ACs were supplied by a local potabilization plant at different age of operation: AC1: new activated carbon; AC2: regenerated activated carbon; AC3: regenerated activated carbon in use at the plant. The status of operation, and the characteristics of the feedstock and the thermal process used to produce the ten chars are summarized in **Table 1**.

Before being characterized and used in isotherm studies, all the char samples were repeatedly washed with ultrapure water according to the ASTM D-5919-96 method.

2.3 Biochar and activated carbon characterization

The chars investigated in this study were physicochemically characterized through the determination of ash content, pH of the point of zero-charge (pH_{pzc}), physisorption analysis, iodine and methylene blue adsorption indexes (I_2In and MBIn), as well as for water-extractable substances of environmental concern. The procedures adopted for the aforementioned determinations are briefly described below, whilst full details are provided in the *Supplementary Material* section. For the determination of the parameters described below, standard methods were used when available.

2.3.1 Ash content

The ash content was determined according to the ASTM International D 2866-11 (American Standard Test Method (ASTM), 2018), which refers to the analysis of ACs.

2.3.2 Water-extractable substances

Metals (namely Sb, As, Cd, Cr, Pb, Hg, Ni and Se), PAHs and PCBs were extracted according to the EN 12902 standard (Comite Europeen de Normalisation (CEN), 2004). After extraction, metals were determined by an Elan 6100 ICP-MS (Perkin Elmer, Waltham, Massachusetts, USA), whereas PAHs and PCBs were preconcentrated by solid-phase extraction (SPE) and analysed by GC-MS, as elsewhere described (Bruzzoniti et al., 2019a; Rivoira et al., 2019). Quality controls were performed to verify the recovery efficiency of PAHs and PCBs during the preconcentration step, using labelled standards, as specified in the *Supplementary material* (see **Tables S1** for BCs and **S2** for ACs).

2.3.3 pH of the point of zero charge

The pH of the point of zero-charge (pH_{pzc}) was determined using the pH drift method, widely adopted for the evaluation of the surface charge of biochars and ACs (Del Bubba et al., 2020).

2.3.4 Adsorption indexes

The determination of I_2In and MBIn was performed according to the definitions indicated by CEFIC for ACs (Conseil Européen des Fédérations de l'Industrie Chimique (CEFIC), 1986).

178 *2.3.5 Physisorption analysis*

179 Physisorption analysis of biochars and ACs was performed via nitrogen adsorption and desorption
180 experiments using a Porosity Analyser Thermo Fisher Scientific (Milan, Italy) model
181 SORPTOMATIC 1990 according to the American Society for Testing and Materials specifications
182 (American Society for Testing and Materials, 2012, 2017). In further detail, the specific surface area
183 (SSA) and micropore surface area (MiSSA) were determined respectively by the Brunauer–Emmett–
184 Teller (BET) method and by t-plot method, whereas mesopore surface area (MeSSA) was measured
185 by the Barrett-Joyner-Halenda (BJH) method applied to desorption data.

186 *2.3.6 Quality control of biochar and activated carbon characterization*

187 Quality control of char characterization measurements was carried out by comparing the results here
188 obtained for AC1 and AC2 with those reported in the technical specifications of the two commercial
189 materials.

190 2.4 Adsorption studies on DIAA and VOCs

191 Adsorption tests were performed on DIAA and VOCs in ultrapure water (pH = 6.5±0.1) using the
192 micro-isotherm technique for adsorbates at ppb concentrations, as established by ASTM D5919-96
193 standard (American Standard Test Method (ASTM), 1996). Aliquots of 40 mL and 100 mL,
194 containing fixed amounts of DIAA and VOCs, respectively (DIAA: 5 µg L^{-1} for BCs and 20 µg L^{-1}
195 for ACs; VOCs: 5 µg L^{-1} or 20 µg L^{-1} for BCs and 20 µg L^{-1} for ACs) were put in contact with
196 different amounts of BCs/ACs varying approximately between 0.02 and 0.5 g. The mixture was
197 stirred in an orbital shaker for 24 hours. The solution was then filtered through a mixed cellulose ester
198 membrane (0.45 µm). Control experiments using the same aforementioned concentrations of target
199 analytes were also conducted without the addition of the adsorbent materials, in order to estimate
200 their removal due to mechanisms other than sorption (e.g. volatilization and degradation).

201 Experimental data were fitted by the Freundlich isotherm model (Foo and Hameed, 2010):

202 $$\log\frac{X}{M}=\log K_F+\frac{1}{n}\log C_e$$

Where X/M is the ratio of the amount of analyte adsorbed per mass unit of sorbent (mg g^{-1}), K_F is the constant of the Freundlich isotherm equation ($mg^{1-1/n}$ $L^{1/n}$ g^{-1}) related to adsorption capacity, C_e is the equilibrium concentration (mg L^{-1}), and 1/n is the exponent of non-linearity.

2.5 Analytical determination of DIAA and VOCs

Residual DIAA concentrations were determined by ion chromatography coupled with triple-stage quadrupole mass spectrometry as elsewhere described (Bruzzoniti et al., 2019b). Residual VOC concentrations were determined by GC-MS after SPE. Details of both procedures are given in the *Supplementary Material Section*.

2.6 Water sample collection and characterization

Water samples were withdrawn from two potabilization plants located in the Piedmont region (North Italy) which treat the same raw water. One sample (labelled as DSB) was taken at the outlet of the dynamic separation basins for the removal of slurry from clarified waters (in which coagulant, hypochlorite and chlorine dioxide solutions are dosed), before entering the activated carbon beds. The other sample (labelled as CB) was taken at the outlet of a clarification basin (in which coagulant only is added), before entering the activated carbon beds. The water samples were characterized for pH and total organic carbon (TOC). TOC was determined using a Shimadzu TOC-V-CSH analyser, by the differential method, i.e. analysing both total carbon (TC) and total inorganic carbon (TIC) through separate measurements and calculating TOC by subtracting TIC from TC.

2.7 Data analysis

Least squares regressions and related analyses of variance (ANOVA) were performed with Excel 2016 (Microsoft, Redmond, WA, USA). Principal component analysis (PCA) and cluster analysis (CA) were carried out using the Minitab statistical software package, version 17.1.0 (Minitab Inc., State College, PA, USA). All data plots were performed using Excel 2016.

3 Results and discussion

3.1 Characterization of chars

3.1.1 Ash content

In biochars, ash percentages were found in the quite wide range of 6-49% (**Table 2**), with the lowest value achieved for BC7, which derived from corn cob under pyrolysis treatment at 450°C (**Table 1**). Ash content in materials intended for water filtration is regulated by EN 12915-1 standard, which sets a limit of 15%, since a high ash content in filtering media is expected to reduce adsorption activity (Inyang and Dickenson, 2015). Hence, as regards this parameter, only BC2, BC3, and as previously mentioned BC7, are allowed to be used as sorbent materials in potabilization facilities.

The data obtained here can be interpreted based on the characteristics of biomass and thermal conversion processes through which the chars were obtained. According to literature, ash concentration of chars is mainly influenced by the type of feedstock, being woody biomass the one providing a lower ash content, compared to other feedstocks, such as non-woody vegetal biomass and animal waste (Tomczyk et al., 2020). However, the type of thermal conversion process (i.e. pyrolysis or gasification) and the temperature and contact time conditions adopted in the process may also play a role in determining the ash concentration, which obviously depends on the amount of char obtained. In this regard, it should be remarked that biochar yield is a function of the type of thermal conversion process (i.e. pyrolysis or gasification) and the temperature and contact time conditions adopted in the process, being the highest yields obtained with pyrolysis conducted at low temperature and high contact time (slow pyrolysis) (Inyang and Dickenson, 2015). Hence, it is evident that, if the same feedstock is used, the ash concentration will be higher in gasification processes than in pyrolysis (Fryda and Visser, 2015). Moreover, increasing ash percentages will be obtained with increasing temperature (Rafiq et al., 2016) and higher ash concentrations will be found under fast pyrolysis conditions (Brewer et al., 2009). Based on these considerations, it makes sense that BC2, BC3, and BC7, all deriving from slow pyrolysis processes (**Table 1**), showed ash percentages much lower than BC5 and BC6, which were conversely obtained under gasification conditions using a same patented process and plant. The very high ash concentration found in BC4 (about 29%) compared to BC3, both produced with the patented PYREG® pyrolysis process under the same experimental conditions,

254 could be attributed to the different nature of the feedstocks employed, i.e. non woody vegetal biomass
255 for BC4 and woody waste biomass for BC3 (**Table 1**). Finally, the unexpected high ash content of
256 BC1 probably depends on the peculiar characteristics of the woody waste used as feedstock, which
257 derives from the cutting of a forest planted for the phytoremediation of a soil contaminated by
258 different chemicals, including heavy metals. Virgin activated carbon (AC1) showed a lower ash
259 content (7%), in agreement with the high standard quality requested by the potabilization plant in its
260 specifications. Higher ash percentages were obviously found in regenerated and in-use ACs (i.e. AC2
261 and AC3).

262 *3.1.2 Water-extractable substances*

263 The thermal conversion process that transforms biomasses into chars may lead to the formation of
264 unwanted organic and inorganic hazardous species, depending on the original composition of the
265 feedstocks. Among them, PAHs (Wang et al., 2017), PCBs (European Biochar Foundation (EBC))
266 and heavy metals (Lievens et al., 2009) can be present in biochars, thus introducing possible limitation
267 in the use of the chars themselves. The EN 12915-1 normative regulates the presence of water
268 extractable pollutants in materials to be applied for water treatments, setting a threshold concentration
269 limit for the sum of six PAH compounds (i.e. fluoranthene, benzo(b)fluoranthene,
270 benzo(k)fluoranthene, benzo(a)pyrene, benzo(g,h,i)perylene and indeno-(1,2,3-cd)-pyrene) at 0.02
271 μg L^{-1}. In addition, the EN standard imposes limits to the presence of As (10 μg L^{-1}), Cd (0.5 μg L^{-1}),
272 Cr (5 μg L^{-1}), Hg (0.3 μg L^{-1}) Ni (15 μg L^{-1}), Pb (5 μg L^{-1}), Sb (3 μg L^{-1}) and Se (3 μg L^{-1}). As
273 regards PCBs, no limit is currently established by the EN standard. However, it should be mentioned
274 that PCB concentrations are regulated in biochars to be used for soil conditioning and feed additives
275 (European Biochar Foundation (EBC); International Biochar Initiative, 2015).

276 Results obtained for leachable PAHs showed that all the chars fulfil the limits set by EN 12915-1
277 regulation. In detail, the regulated PAHs were detected in BC1, BC2, BC3, BC4, and BC7 (all
278 deriving from pyrolysis), with the sum of their concentrations ranging from 1.6 ng L^{-1} (BC4) to 13.3

279 ng L^{-1} (BC7). Conversely, for ACs and the other BCs, the concentrations of PAHs included in the EN
280 standard were below detection limits (**Table S3** of the *Supplementary material*).
281 EPA PAHs other than the ones included in the EN standards were also determined (see **Table S3**),
282 highlighting that PAHs with 2-3 aromatic rings were generally more abundant than those with higher
283 molecular weight, as also observed elsewhere (Lyu et al., 2016). BC7, which was produced under
284 pyrolysis at the lowest temperature (450°C), was the material providing by far the highest total
285 leachable PAH concentration (826 ng L^{-1}), while biochars obtained under gasification conditions
286 showed the lowest PAHs release (11-12 ng L^{-1}). These BCs were also the ones providing respectively
287 the highest and the lowest benzo(a)pyrene equivalent concentrations ($BaPy_{eq}$), based on toxic
288 equivalence factors (TEFs) available in literature (Berardi et al., 2019). PAHs occurrence in BCs can
289 be explained based on re-polymerization phenomena of the radical hydrocarbon fragments formed
290 during the thermal process, which are favoured by the absence of oxygen. Moreover, the presence of
291 PAHs depends also on the conversion temperature adopted, which plays a main role in PAH
292 formation up to about 500°C, but also in their degradation beyond this value (Parker et al., 2014; Lyu
293 et al., 2016). An influence of the biomass composition in the presence of leachable PAHs can also be
294 evidenced from the comparison of BC3 (321 ng L^{-1}) and BC4 (26 ng L^{-1}), which were obtained under
295 exactly the same pyrolysis conditions, but with completely different feedstocks.
296 The concentrations of extractable PCBs found in the BCs and ACs leachate are reported in **Table S4**
297 of the *Supplementary material*. BC1 was the only char exhibiting the presence of all the PCBs
298 investigated in its leachate, with total concentration of about 96 ng L^{-1}. Conversely, all the other BCs
299 showed PCB15 as the only leachable chlorinated biphenyl, the concentration of which was in the low
300 ng L^{-1} range (0.56-2.8 ng L^{-1}) in BC2, BC3, and BC4 and about one order of magnitude higher (21.7-
301 29 ng L^{-1}) in BC5 and BC6. PCBs occurrence in the BC leachate could be ascribed to the thermal
302 transformation of chloride, originally contained in feedstocks (Reed) and in this regard, it should be
303 recalled that BC1 has been prepared with wood waste deriving from a multi-contaminated soil. To

304 the best of our knowledge, this is the first study investigating PCBs in BC leachates, thus preventing
305 any comparison with literature data.
306 The concentrations of metals determined in BC leachates are illustrated in **Table S5** of the
307 *Supplementary material*, where the limits set by UNI EN 12915-1 are also reported. BCs generally
308 complied with the release limits set by the aforementioned regulation, with the only exception of
309 BC1, which exceeded the limit for Cr, with an observed concentration (17.3 μg L^{-1}) three times higher
310 than this limit, in agreement with the considerations previously reported. As regards ACs, only AC3
311 exceeded limit for Se (5 μg L^{-1} versus 3 μg L^{-1}, see **Table S5**), suggesting that a possible saturation
312 of adsorption sites occurred during service.
313 *3.1.3 pH of the point of zero charge*
314 The values of pH_{pzc} were characterized by a high variability (7.0-12.0), in agreement with the wide
315 range of the production conditions, including the type of feedstock that, as already reported in
316 literature, significantly influence this property (Ippolito et al., 2020). For BCs, a significant linear
317 correlation with positive slope was found by plotting ash concentrations as a function of pH_{pzc} values
318 (R^2 = 0.780, P<0.05). This correlation can be ascribed to the ash composition typically reported in
319 literature (Ippolito et al., 2020), which mainly consists in metals present in the hydroxide form, thus
320 promoting the increase of the pH in solution. ACs did not follow this trend, as the higher the amount
321 of ash, the lower the pH_{pzc} observed. This finding is in agreement with the increasing amount of
322 chemicals other than organic carbon adsorbed by ACs during operation, which however do not
323 influence the alkalinity of material surfaces.
324 The measurement of the pH_{pzc} values allowed us to make some considerations about the net surface
325 charge of the chars, which mainly depends on the surface functional groups of the material and is
326 extremely useful to explain the adsorption behaviours of BCs towards ionized or ionisable
327 compounds. Most BCs (with the only exception of BC7) exhibited pH_{pzc} higher than pH values of
328 drinking water collected before entering AC filters of the aforementioned potabilization plants, which
329 ranged between 7.6 and 7.7. Hence, BC1-BC6 are expected to exhibit positively charged surfaces

330 when they were applied to the treatment of these waters, whereas BC7 is supposed to be negatively
331 charged (Li et al., 2017).
332 *3.1.4 Adsorption indexes of chars*
333 The adsorption efficiency of the BCs was evaluated in comparison with ACs through the
334 determination of I_2In and MBIn (**Table 2**).
335 I_2In is commonly considered as related to the presence in the structure of micropores (average
336 diameter less than 2 nm) and should be therefore informative for the removal efficiency of small-size
337 organic water pollutants (Del Bubba et al., 2020). Conversely, MBIn should be associated to the
338 abundance of mesopores (average diameter in the range 2-50 nm) and thus considered as a useful
339 indicator of adsorption capacity towards medium-large sized organic pollutants (Del Bubba et al.,
340 2020). For BCs, the I_2In was found in the range 77-197 mg I_2 g^{-1}, with BCs obtained from gasification
341 (i.e. BC5 and BC6) showing the highest values (156-197 mg I_2 g^{-1}), while the lowest ones (77-88 mg
342 I_2 g^{-1}) were exhibited by materials produced under pyrolytic conditions (i.e. BC3 and BC7). The range
343 determined for I_2In in BCs was about five times lower than that determined in virgin and regenerated
344 ACs (i.e. AC1 and AC2), ranging between 540 and 1010 mg I_2 g^{-1}. As expected, the I_2In of AC3 (i.e.
345 AC2 after some use in the potabilization plant) was lower than that of AC2 (438 mg I_2 g^{-1}), in
346 agreement with the progressive pore saturation phenomena occurring during operation.
347 The MBIn showed a trend within the BCs and ACs clusters, and among them, similar to that described
348 for I_2In (e.g. higher values for ACs than BCs and for BC5 and BC6 compared to the other BCs).
349 Accordingly, as illustrated by **Figure S1** of the *Supplementary material*, the two indexes showed a
350 very good linear correlation (R^2 = 0.945, P<<0.05), in agreement with findings observed elsewhere
351 for different types of ACs and BCs (Del Bubba et al., 2020), even though a lower determination
352 coefficient was observed by excluding ACs from the correlation (R^2= 0.534, P=0.062). The much
353 lower correlation was mainly ascribable to the opposite trend observed for some pairs of materials,
354 such as BC5 and BC6, the latter exhibiting lower MBIn but higher I_2In than the former. These findings

355 can be explained by the general differences in micro, meso, and macroporosity distributions of BCs
356 due to the different experimental conditions adopted for their production.

357 *3.1.5 Physisorption analysis*

358 **Table 2** illustrated the results obtained for the porosimetry analyses (i.e. BET SSA, t-plot MiSSA and
359 BJH desorption cumulative MeSSA) of the investigated BCs and ACs.

360 As expected, ACs exhibited much higher values of the SSA (561-1053 m^2 g^{-1}) than BCs (136-309 m^2
361 g^{-1}), being the latter group characterized by a data trend similar to those observed for adsorption
362 indexes. To elaborate, BC5 and BC6, in addition to showing greater values of the adsorption indexes,
363 also exhibited the highest SSA, whereas BC7 had the lowest values of the aforementioned parameters.
364 These findings can be explained by the well-recognized role of temperature in increasing the surface
365 area (Liu et al., 2010; Ahmad et al., 2014), since BC5/BC6 and BC7 were obtained by the highest
366 and lowest conversion temperature, respectively (**Table 1**). Indeed, very good linear correlations (R^2
367 = 0.981-0.984, $P<<0.05$) were observed between SSA and adsorption indexes (see **Figures S2-A** and
368 **S2-B** of the *Supplementary material*), even excluding ACs from the regression (R^2 = 0.781-0.904,
369 data not shown).

370 In general, BCs showed a higher percentage of macroporosity than ACs. However, it should be noted
371 that BC3 and BC4, produced with the same patented PYREG® pyrolysis system, had a very small
372 microporosity, comparable to that observed in ACs. The relative percentages of microporosity and
373 mesoporosity were comparable in all materials, with the exception of AC1, which was strongly
374 characterized by microporosity. Moreover, high correlations were found between MiSSA and I_2In
375 (R^2 = 0.972, $P<<0.05$), as well as between the MeSSA and MBIn (R^2 = 0.922, $P<<0.05$) (**Figs. S2-C**
376 **and S2-D**). However, similarly to findings observed for the correlation between adsorption indexes,
377 also these relationships were mainly driven by the presence of ACs, since their exclusion strongly
378 lowered the determination coefficients, making null the significance of the correlation (data not
379 shown).

Differently from adsorption indexes, SSA is often reported as fundamental parameter for the characterization of sorption properties of BCs. In order to understand the overall significance of SSA data obtained here, it is therefore interesting to compare them with the values reported in literature for the numerous biochars obtained from vegetal feedstocks. However, the kind of conversion process, its temperature and time, as well as the type of biomass used, strongly affects the SSA of BCs. Accordingly, this comparison was restricted to biochars obtained from woody vegetal feedstocks, which represent the main type of biomass used for the production of BCs here investigated, obtaining SSA values in the range 2-637 $m^2 g^{-1}$ (Chen et al., 2016; Hansen et al., 2016; Chen et al., 2019; Grojzdek et al., 2021). Therefore, the SSA values between 136 and 309 $m^2 g^{-1}$ measured in this study are fully in the range reported in the literature.

3.2 Principal component analysis of the char characterization parameters

To summarize the wide group of information discussed above, deriving from the determination of the several characterization parameters in the ten char samples, a multivariate elaboration of the autoscaled original data was performed by means of PCA. In more detail, PCA elaboration included the following eleven parameters: conversion temperature (T), the seven parameters reported in **Table 2** (i.e. ash, pH_{pzc}, SSA, MiSSA, MeSSA, I_2In, and MBIn), total PAHs (expressed as BaPy TEF concentrations), total PCBs, and total metals. Three principal components (PCs), characterized by eigenvalues > 1 and accounting for percentages of explained variances (E.V.) of 54.9%, 26.4%, and 11.0%, were obtained (total E.V. = 92.3%). **Figure 1** illustrates the plots of scores (**Fig. 1A-B**) and loadings (**Fig. 1C-D**) of PC1 versus PC2 and PC1 versus PC3, which represent E.V. of 81.3% and 65.9%, respectively. The contributions of each variable to the three significant PCs were not always well differentiated, even though most original variables showed remarkably different absolute values of loadings among the three components. In more detail, SSA, MiSSA, MeSSA, I_2In, and MBIn contributed mainly in PC1, pH_{pzc} and above all ash were mainly represented on PC2, whilst total PCBs exhibited by far the highest loading on PC3. Conversely, T was represented in PC1 and PC3 to the same extent, whereas total PAHs and metals contributed almost equally to PC2 and PC3. Among

406 the ten investigated chars, ACs clustered in both score plots, mainly due to their peculiar
407 characteristics in terms of adsorption indexes and physisorption data. BC5 and BC6, which derived
408 from the same gasification process, also clustered in both score plots mostly because of the
409 particularly high values of ash and very low leachable concentrations of total PAHs. Actually, BC6
410 was the closest char to the AC cluster, suggesting interesting adsorption properties. This consideration
411 points out that PCA is a valuable tool to select the best sorbents for adsorption measurements, when
412 one or more reference materials are included in the unsupervised multivariate analysis as
413 comparators. BC2, BC3, and BC4 identified a further cluster in both score plots. Conversely, BC1
414 and BC7 behaved as outliers, being they quite distant from the other BCs and the farthest from ACs,
415 due to their peculiar values of the coordinates on PC2 and PC3. In fact, their scores, were mainly
416 governed by the concentration values of ash (the highest in BC1 and the lowest in BC7), total PAHs
417 (intermediate value for BC1 and the highest one for BC7), and total metals (the highest in BC1 and
418 the lowest in BC7), which strongly contributed to these PCs.
419 In order to have a quantitative confirmation of the findings of PCA, CA was carried out, by using the
420 complete linkage method and the Euclidean distances on the autoscaled values of the aforementioned
421 eleven variables (**Figure 2**). The dendrogram confirmed the results of PCA, especially for BC2, BC3,
422 and BC4, for BC5 and BC6, and for AC1 and AC2, which were grouped in three clusters at similarity
423 percentages higher than 75%. It is also worth noting that BC5 and BC6 clustered with AC2 and AC3
424 with a similarity of about 50%. CA also highlighted the high distance between the virgin activated
425 carbon (AC1) and the regenerated ones (AC1 and AC2), which exhibited a very low degree of
426 similarity (about 20%).
427 Based on the results of the multivariate characterization of BCs and ACs and their summarising
428 picture obtained by PCA and CA, BC6 and BC7 were selected for the successive adsorption studies,
429 as the closest and the farthest materials to the ACs cluster, respectively. Within this latter group, the
430 virgin (AC1) and the regenerated (AC2) activated carbon were chosen as comparators.
431 3.3 Adsorption studies on DIAA and VOCs

Adsorption isotherm experiments were performed on BC6, BC7, AC1, and AC2, using the anion DIAA and the neutral VOCs benzene and 1,2-dichlorobenzene in order to (i) hypothesize possible retention mechanisms of BCs (Inyang and Dickenson, 2015) and (ii) estimate sorption capacity of chars towards these pollutants, which are of environmental concern, *per se*.

3.3.1 DIAA

As regards DIAA, at 5 µg/L, both ACs exhibited a quantitative removal for all the char concentrations tested, since target analyte was not detected in water solutions after 24 h of contact. Conversely, removal in the ranges of 18.8-70.8 % and 5.1-28.4% were observed for BC6 and BC7, respectively (**Table 3**). The different adsorption performances exhibited by BC6 and BC7 should be ascribed not only to the different surface area, but also to the surface charge, as derived by pH_{pzc} measures. In fact, pH_{pzc} tests indicated a significantly higher positive surface charge for BC6 (pH_{pzc}=11.0) than BC7 (pH_{pzc}=7.0) at the working pH value (pH=6.5), which is responsible for electrostatic interactions between biochar and DIAA (Inyang and Dickenson, 2015).

As no detectable DIAA concentrations were found for ACs at 5 µg L^{-1}, adsorption isotherm experiments were repeated using an initial concentration of 20 µg L^{-1}. With this concentration, the removal percentage of the two ACs remained quite similar, ranging approximately from about 89 % to 100 % in both cases (**Table 3**). As illustrated by **Figure 3**, adsorption data were fitted by the linearized Freundlich equation, observing in all cases determination coefficients ≥ 0.925 and statistically significant models based on ANOVA (*P*-values << 0.05). Values of K_F (**Table 3**) for BCs were about three orders of magnitude lower than those for ACs. Hence, BCs provided a poor adsorption ability compared to those determined for materials routinely used in water treatment plants. In more detail, based on the K_F values, BC6 exhibited sorption ability about 3 times higher than BC7. A similar efficiency ratio was observed for AC1 vs. AC2, in accordance with the fact that the former is a virgin material, while the latter is a regenerated char. Slope (1/n) values of the regression lines (**Fig. 3**) were in all cases < 1 (from 0.432 for BC7 to 0.736 for AC1), following the order BC7≈BC6<<AC2<AC1. The values determined for slopes suggest an L-type isotherm

458 behaviour (European Centre for Ecotoxicology and Toxicology of Chemicals (ECETOC), 2013) for
459 the adsorption of DIAA on the investigated chars, notwithstanding the pseudo-linear aspect of the
460 experimental equilibrium concentration data (i.e. X/M vs. Ce), which is probably related to the quite
461 high concentrations of material and their narrow range tested here (i.e. about one order of magnitude).
462 This means that when DIAA concentration increases, the relative adsorption decreases due to the
463 saturation of adsorption sites available to DIAA, resulting in relatively less intense adsorption, with
464 increasing the amount of chemical adsorbed onto the material, as commonly observed for the sorption
465 of organic compounds on chars.

466 *3.3.2 VOCs*

467 Adsorption isotherm experiments on VOCs showed a not negligible variability of data, probably due
468 to the high vapour pressure and low water solubility of these analytes (Henry constants of $5.5 \cdot 10^{-4}$
469 and $2.3 \cdot 10^{-3}$ atm·m^3 mol^{-1}, for benzene and 1,2-dichlorobenzene, respectively). In this regard, it
470 should be noted that control experiments evidenced losses of both the investigated VOCs (about 15-
471 25%). Accordingly, adsorption isotherms were not calculated for VOCs. However, it is possible to
472 state that both BCs showed good adsorption properties, since, at both 20 and 5 µg/L the removal
473 percentage was almost quantitative for ACs and BC6, and approximately equal to 60-70% and 70-
474 80%, for BC7 towards benzene and 1,2-dichlorobenzene, respectively.

475 3.4 Removal tests in water samples collected in drinking water plants

476 The removal capabilities of BC6 and BC7 were additionally tested in two water samples (i.e. DSB
477 and CB) collected from the drinking water plant treatment train (before entering the final refinement
478 stage with activated carbon beds) and compared with those of commercial AC1. These tests were
479 performed by putting in contact for 24 h 0.4 g of chars with 100 mL of DSB and CB spiked with 20
480 µg L^{-1} of DIAA or VOCs. In such a way, the possible competitive effects exhibited by the matrix can
481 be assessed and results obtained from adsorption experiments in ultrapure water eventually
482 confirmed. To better explain possible competitions mechanisms, Total Organic Carbon (TOC) was
483 initially measured in the two samples, obtaining TOC values of 4.3 mg L^{-1} and 2.4 mg L^{-1} for CB and

DSB, respectively. The lower TOC value observed for DSB should be ascribed to the disinfection stage operated in this treatment train. The results obtained in these removal tests are summarized in **Table 4**. As a general consideration, the use of water samples collected within the treatment train of the potabilization plants did not alter the performance of the BCs, even though the lower performances of biochars compared to the activated carbon were confirmed. Results obtained in real water samples fully support the design of column experiments to assess accurately the removal capacity and exhausting time of BCs, with particular reference to BC6.

4 Conclusions

Within the actions pursued in a circular economy approach fostered by European Union for waste management, the reuse of waste is promoted for the reduction of resources consumption. Biochar is one successful example of valorisation of wastes.

In this paper, seven BCs obtained from gasification or pyrolysis processes of waste vegetal biomass, were characterized in depth for numerous parameters, in comparison with a virgin commercial AC, a freshly regenerated AC, and a regenerated AC in use at a potabilization facility. The characterization included the evaluation of "environmental concern" parameters (e.g. PAHs and metals release), for which mandatory limits are provided at European level for materials intended as sorbents for drinking water filtration, but seldom evaluated elsewhere. Most BCs met these limits, whilst the "sorption performance parameters" regulated in the European standard (i.e. I_2In and ash in the UNI EN 12915-1) were in almost all cases outside the acceptance thresholds, suggesting lower efficiencies compared to ACs. However, the sorption ability of a given material towards a specific molecule is the result of a set of characteristics, which all contribute together to the overall removal efficiency, thus suggesting the importance of following a multivariate approach. Indeed, multivariate analyses performed in this work (i.e. PCA and CA) allowed for easily identifying the materials with the closest (BC5 and BC6) or the farthest (BC1 and BC7) characteristics to those of ACs. Accordingly, the multivariate approach should be promoted in the exploration of data deriving from material characterization, rather than the evaluation of individual characteristics, even if they are regulated by legislation.

Adsorption tests towards DIAA and VOCs carried out in ultrapure water highlighted the much lower sorption ability of BC7 compared to BC6. These results were in agreement with findings of multivariate analyses, therefore suggesting intermediate sorption performances for BC1-BC5. Interestingly, removal tests in waters withdrawn from potabilization plants did not evidence any significant decrease of the sorption ability of BC6 and BC7 towards the investigated contaminants compared to tests in ultrapure water, thus supporting the implementation of column experiments for establishing the maximum loading capacity of the materials in experimental conditions more similar to the real scale.

Even though the sorption performances of BCs are much lower than those of ACs, it should be noted that BCs did not undergo any physical or chemical activation process, which can surely improve their removal capacity. Moreover, the management of waste biomass to produce biochar as adsorbent for water treatment may be regarded as a ‘‘win–win’’ solution for pursuing circular economy principles and protecting the environment.

Acknowledgements

M.C. is grateful to SMAT for the scholarship granted. M.C.B. is grateful to Dr. M. Minella (University of Torino) for TOC measurements and to Prof. C. Sarzanini for fruitful discussion. Financial support from Regione Piemonte (POR-FESR 2014/2020, BIOENPRO4TO 333-148) and from Ministero dell’Università e della Ricerca (MUR) is gratefully acknowledged. The authors would like to thank PYREG GmbH, Romana Maceri Centro Italia S.r.l., Agrindustria Tecco S.r.l., and Sea Marconi s.a.s. for donating the biochars used in this study.

References

Ahmad, M., Rajapaksha, A.U., Lim, J.E., Zhang, M., Bolan, N., Mohan, D., Vithanage, M., Lee, S.S., Ok, Y.S., 2014. Biochar as a sorbent for contaminant management in soil and water: A review. Chemosphere 99, 19-33.

Ali, I., Gupta, V., 2006. Advances in water treatment by adsorption technology. Nature protocols 1, 2661.

American Society for Testing and Materials, 2012. Standard Test Method for Carbon Black—Total and External Surface Area by Nitrogen Adsorption (ASTM-D6556-10). ASTM International, West Conshohocken, PA.
American Society for Testing and Materials, 2017. Standard Practice for Calculation of Pore Size Distributions of Catalysts and Catalyst Carriers from Nitrogen Desorption Isotherms (ASTM-D4641-17). ASTM International, West Conshohocken, PA.
American Standard Test Method (ASTM), 1996. D 5919-96 Standard Practice for Determination of Adsorptive Capacity of Activated Carbon by a Micro-Isotherm Technique for Adsorbates at ppb Concentrations.
American Standard Test Method (ASTM), 2018. D2866-11 Standard Test Method for Total Ash Content of Activated Carbon.
Berardi, C., Fibbi, D., Coppini, E., Renai, L., Caprini, C., Scordo, C.V.A., Checchini, L., Orlandini, S., Bruzzoniti, M.C., Del Bubba, M., 2019. Removal efficiency and mass balance of polycyclic aromatic hydrocarbons, phthalates, ethoxylated alkylphenols and alkylphenols in a mixed textile-domestic wastewater treatment plant. Science of The Total Environment 674, 36-48.
Brewer, C.E., Schmidt-Rohr, K., Satrio, J.A., Brown, R.C., 2009. Characterization of biochar from fast pyrolysis and gasification systems. Environmental Progress & Sustainable Energy 28, 386-396.
Bruzzoniti, M.C., Appendini, M., Rivoira, L., Onida, B., Del Bubba, M., Jana, P., Sorarù, G.D., 2018. Polymer-derived ceramic aerogels as sorbent materials for the removal of organic dyes from aqueous solutions. Journal of the American Ceramic Society 101, 821-830.
Bruzzoniti, M.C., Rivoira, L., Castiglioni, M., El Ghadraoui, A., Ahmali, A., El Mansour, T.E.H., Mandi, L., Ouazzani, N., Del Bubba, M., 2019a. Extraction of Polycyclic Aromatic Hydrocarbons and Polychlorinated Biphenyls from Urban and Olive Mill Wastewaters Intended for Reuse in Agricultural Irrigation. Journal of AOAC International.
Bruzzoniti, M.C., Rivoira, L., Meucci, L., Fungi, M., Bocina, M., Binetti, R., Castiglioni, M., 2019b. Towards the revision of the drinking water directive 98/83/EC. Development of a direct injection ion chromatographic-tandem mass spectrometric method for the monitoring of fifteen common and emerging disinfection by-products along the drinking water supply chain. Journal of Chromatography A 1605, 360350.
Cao, X., Harris, W., 2010. Properties of dairy-manure-derived biochar pertinent to its potential use in remediation. Bioresource Technology 101, 5222-5228.
Castiglioni, M., Rivoira, L., Ingrando, I., Del Bubba, M., Bruzzoniti, M.C., 2021. Characterization techniques as supporting tools for the interpretation of biochar adsorption efficiency in water treatment: a critical review. Molecules 26, 5063, 1-22.
Chen, D., Chen, X., Sun, J., Zheng, Z., Fu, K., 2016. Pyrolysis polygeneration of pine nut shell: Quality of pyrolysis products and study on the preparation of activated carbon from biochar. Bioresource Technology 216, 629-636.
Chen, W., Wei, R., Yang, L., Yang, Y., Li, G., Ni, J., 2019. Characteristics of wood-derived biochars produced at different temperatures before and after deashing: Their different potential advantages in environmental applications. Science of The Total Environment 651, 2762-2771.
Colantoni, A., Evic, N., Lord, R., Retschitzegger, S., Proto, A.R., Gallucci, F., Monarca, D., 2016. Characterization of biochars produced from pyrolysis of pelletized agricultural residues. Renewable and Sustainable Energy Reviews 64, 187-194.
Comite Europeen de Normalisation (CEN), 2004. EN 12902:2004 Products used for treatment of water intended for human consumption - Inorganic supporting and filtering materials - Methods of test.
Comite Europeen de Normalisation (CEN), 2009. EN 12915-1:2009 Products used for the treatment of water intended for human consumption. Granular activated carbon. Virgin granular activated carbon.

Conseil Européen des Fédérations de l'Industrie Chimique (CEFIC), 1986. Test Methods for Activated Carbon, available at https://acpa.cefic.org/images/Test_method_for_Activated_Carbon_86.pdf.

Del Bubba, M., Anichini, B., Bakari, Z., Bruzzoniti, M.C., Camisa, R., Caprini, C., Checchini, L., Fibbi, D., El Ghadraoui, A., Liguori, F., Orlandini, S., 2020. Physicochemical properties and sorption capacities of sawdust-based biochars and commercial activated carbons towards ethoxylated alkylphenols and their phenolic metabolites in effluent wastewater from a textile district. Science of the Total Environment.

European Biochar Foundation (EBC), EBC (2012) European Biochar Certificate - Guidelines for a Sustainable Production of Biochar. Arbaz, Switzerland. http://www.europeanbiochar.org/en/download. Version 8.2E of 19th April 2019, DOI: 10.13140/RG.2.1.4658.7043.

European Centre for Ecotoxicology and Toxicology of Chemicals (ECETOC), 2013. Environmental exposure assessment of ionisable organic compounds, Technical Report No. 123. Brussels.

European Commission, 2010. Water Framework Directive, ENV 09-018, https://ec.europa.eu/environment/pubs/pdf/factsheets/water-framework-directive.pdf.

Foo, K.Y., Hameed, B.H., 2010. Insights into the modeling of adsorption isotherm systems. Chemical engineering journal 156, 2-10.

Fryda, L., Visser, R., 2015. Biochar for Soil Improvement: Evaluation of Biochar from Gasification and Slow Pyrolysis. Agriculture 5, 1076-1115.

Grojzdek, M., Novosel, B., Klinar, D., Golob, J., Gotvajn, A.Ž., 2021. Pyrolysis of different wood species: influence of process conditions on biochar properties and gas-phase composition. Biomass Conversion and Biorefinery, 1-11.

Gwenzi, W., Chaukura, N., Noubactep, C., Mukome, F.N.D., 2017. Biochar-based water treatment systems as a potential low-cost and sustainable technology for clean water provision. Journal of Environmental Management 197, 732-749.

Han, J., Zhang, X., 2018. Evaluating the Comparative Toxicity of DBP Mixtures from Different Disinfection Scenarios: A New Approach by Combining Freeze-Drying or Rotoevaporation with a Marine Polychaete Bioassay. Environmental Science & Technology 52, 10552-10561.

Han, J., Zhang, X., Jiang, J., Li, W., 2021. How Much of the Total Organic Halogen and Developmental Toxicity of Chlorinated Drinking Water Might Be Attributed to Aromatic Halogenated DBPs? Environmental Science & Technology 55, 5906-5916.

Hansen, V., Müller-Stöver, D., Munkholm, L.J., Peltre, C., Hauggaard-Nielsen, H., Jensen, L.S., 2016. The effect of straw and wood gasification biochar on carbon sequestration, selected soil fertility indicators and functional groups in soil: an incubation study. Geoderma 269, 99-107.

Hou, Y., Chu, W., Ma, M., 2012. Carbonaceous and nitrogenous disinfection by-product formation in the surface and ground water treatment plants using Yellow River as water source. Journal of Environmental Sciences 24, 1204-1209.

International Biochar Initiative, 2015. Standardized Product Definition and Product Testing Guidelines for Biochar That Is Used in Soil available at https://www.biochar-international.org/wp-content/uploads/2018/04/IBI_Biochar_Standards_V2.1_Final.pdf.

Inyang, M., Dickenson, E., 2015. The potential role of biochar in the removal of organic and microbial contaminants from potable and reuse water: A review. Chemosphere 134, 232-240.

Ippolito, J.A., Cui, L., Kammann, C., Wrage-Mönnig, N., Estavillo, J.M., Fuertes-Mendizabal, T., Cayuela, M.L., Sigua, G., Novak, J., Spokas, K., Borchard, N., 2020. Feedstock choice, pyrolysis temperature and type influence biochar characteristics: a comprehensive meta-data analysis review. Biochar 2, 421-438.

Jana, P., Bruzzoniti, M.C., Appendini, M., Rivoira, L., Del Bubba, M., Rossini, D., Ciofi, L., Sorarù, G.D., 2016. Processing of polymer-derived silicon carbide foams and their adsorption capacity for non-steroidal anti-inflammatory drugs. Ceramics International 42, 18937-18943.

637 Jiang, J., Han, J., Zhang, X., 2020. Nonhalogenated Aromatic DBPs in Drinking Water Chlorination:
638 A Gap between NOM and Halogenated Aromatic DBPs. Environmental Science & Technology
639 54, 1646-1656.
640 Jiang, J., Zhang, X., Zhu, X., Li, Y., 2017. Removal of Intermediate Aromatic Halogenated DBPs by
641 Activated Carbon Adsorption: A New Approach to Controlling Halogenated DBPs in
642 Chlorinated Drinking Water. Environmental Science & Technology 51, 3435-3444.
643 Kyzas, G.Z., Matis, K.A., 2015. Nanoadsorbents for pollutants removal: A review. Journal of
644 Molecular Liquids 203, 159-168.
645 Lahaniatis, E.S., Bergheim, W., Kotzias, D., Pilidis, G., 1994. Formation of chlorinated hydrocarbons
646 by water chlorination. Chemosphere 28, 229-235.
647 Li, H., Dong, X., da Silva, E.B., de Oliveira, L.M., Chen, Y., Ma, L.Q., 2017. Mechanisms of metal
648 sorption by biochars: Biochar characteristics and modifications. Chemosphere 178, 466-478.
649 Lievens, C., Carleer, R., Cornelissen, T., Yperman, J., 2009. Fast pyrolysis of heavy metal
650 contaminated willow: Influence of the plant part. Fuel 88, 1417-1425.
651 Liu, Z., Zhang, F.-S., Wu, J., 2010. Characterization and application of chars produced from pinewood
652 pyrolysis and hydrothermal treatment. Fuel 89, 510-514.
653 Lyu, H., He, Y., Tang, J., Hecker, M., Liu, Q., Jones, P.D., Codling, G., Giesy, J.P., 2016. Effect of
654 pyrolysis temperature on potential toxicity of biochar if applied to the environment.
655 Environmental pollution 218, 1-7.
656 Martínez, E., Lacorte, S.l., Llobet, I., Viana, P., Barceló, D., 2002. Multicomponent analysis of volatile
657 organic compounds in water by automated purge and trap coupled to gas chromatography–mass
658 spectrometry. Journal of Chromatography A 959, 181-190.
659 McHenry, M.P., 2010. Carbon-based stock feed additives: a research methodology that explores
660 ecologically delivered C biosequestration, alongside live weights, feed use efficiency, soil
661 nutrient retention, and perennial fodder plantations. Journal of the Science of Food and
662 Agriculture 90, 183-187.
663 Méndez, A., Cárdenas-Aguiar, E., Paz-Ferreiro, J., Plaza, C., Gascó, G., 2017. The effect of sewage
664 sludge biochar on peat-based growing media. Biological Agriculture & Horticulture 33, 40-51.
665 Palansooriya, K.N., Yang, Y., Tsang, Y.F., Sarkar, B., Hou, D., Cao, X., Meers, E., Rinklebe, J., Kim,
666 K.-H., Ok, Y.S., 2020. Occurrence of contaminants in drinking water sources and the potential
667 of biochar for water quality improvement: A review. Critical Reviews in Environmental
668 Science and Technology 50, 549-611.
669 Parker, D.S., Kaiser, R.I., Troy, T.P., Ahmed, M.J.A.C.I.E., 2014. Hydrogen abstraction/acetylene
670 addition revealed. Angewandte Chemie International Edition 53, 7740-7744.
671 Perrich, J.R., 2018. Activated carbon adsorption for wastewater treatment. CRC press.
672 Rafiq, M.K., Bachmann, R.T., Rafiq, M.T., Shang, Z., Joseph, S., Long, R., 2016. Influence of
673 pyrolysis temperature on physico-chemical properties of corn stover (Zea mays L.) biochar and
674 feasibility for carbon capture and energy balance. PloS one 11, e0156894.
675 Reed, K.W.a.D., IBI White Paper, Implications and Risks of Potential Dioxin Presence in Biochar,
676 available at https://biochar-international.org/ibi-publications/.
677 Rivoira, L., Appendini, M., Fiorilli, S., Onida, B., Del Bubba, M., Bruzzoniti, M.C., 2016.
678 Functionalized iron oxide/SBA-15 sorbent: investigation of adsorption performance towards
679 glyphosate herbicide. Environmental science and pollution research international 23, 21682-
680 21691.
681 Rivoira, L., Castiglioni, M., Kettab, A., Ouazzani, N., Al-Karablieh, E., Boujelben, N., Fibbi, D.,
682 Coppini, E., Giordani, E., Del Bubba, M., Bruzzoniti, M.C., 2019. Impact of effluents from
683 wastewater treatments reused for irrigation: Strawberry as case study. Environmental
684 Engineering and Management Journal 18, 2133-2143.
685 Singh, B., Singh, B.P., Cowie, A.L., 2010. Characterisation and evaluation of biochars for their
686 application as a soil amendment. Soil Research 48, 516-525.

687 Tomczyk, A., Sokołowska, Z., Boguta, P., 2020. Biochar physicochemical properties: pyrolysis
688 temperature and feedstock kind effects. Reviews in Environmental Science and
689 Bio/Technology 19, 191-215.
690 Wang, C., Wang, Y., Herath, H., 2017. Polycyclic aromatic hydrocarbons (PAHs) in biochar–Their
691 formation, occurrence and analysis: A review. Organic Geochemistry 114, 1-11.
692 Wang, X., Guo, Z., Hu, Z., Zhang, J., 2020. Recent advances in biochar application for water and
693 wastewater treatment: a review. PeerJ 8, e9164-e9164.
694 Wang, Y., Hu, Y., Zhao, X., Wang, S., Xing, G., 2013. Comparisons of Biochar Properties from Wood
695 Material and Crop Residues at Different Temperatures and Residence Times. Energy & Fuels
696 27, 5890-5899.
697 World Health Organization, 2017. Guidelines for drinking-water quality, available at
698 https://apps.who.int/iris/bitstream/handle/10665/254637/9789241549950-
699 eng.pdf?sequence=1&isAllowed=y.

700

Table 1 – Status of operation and production conditions of biochars (BC) and commercial activated carbons (AC); n.a. = not available

Sample	Status	Feedstock	Thermal treatment	Temperature (°C)	Contact time (min)
BC1	Virgin	Wood waste mixture [a]	Pyrolysis	550	10
BC2	Virgin	Wood waste mixture [b]	Pyrolysis	550	10
BC3	Virgin	Wood waste mixture [b]	Pyrolysis	550-600	15
BC4	Virgin	Herbal pomace	Pyrolysis	550-600	15
BC5	Virgin	Wood waste mixture [c]	Gasification	800-900	10
BC6	Virgin	Wood waste mixture [d]	Gasification	800-900	10
BC7	Virgin	Corn cob	Pyrolysis	450	30
AC1	Virgin	Coconut	Pyrolysis+physical activation	800-950	n.a
AC2	Regenerated	Coconut	Pyrolysis+physical activation	800-950	n.a
AC3	In use	Coconut	Pyrolysis+physical activation	800-950	n.a

[a] Composition: 100% Poplar; [b] Unknown composition; [c] Approximate composition: Pine 60%, Beech 25%, Hazel 15%; [d] Approximate composition: Pine 40%, Beech 30%, Hazel 20%, Spruce 10%

Table 2 – Ash (%), pH of the point of zero charge (pH_{pzc}), specific surface area (SSA, BET method, $m^2\ g^{-1}$), surface area of micropores (MiSSA, t-plot method, $m^2\ g^{-1}$), surface area of mesopores (MeSSA, BJH model – desorption cumulative surface area, $m^2\ g^{-1}$), iodine index (I_2In, mg g^{-1}), and methylene blue index (MBIn, mg g^{-1}), determined in biochars (BCs) and activated carbons (ACs). For the parameters tested by replicated analyses (n=3), mean and standard deviations (in bracket) are reported. Available limits set by European regulation EN 12915-1 are also reported; n.a. = not available.

Sample	**Ash**	**pH_{pzc}**	**SSA**	**MiSSA**	**MeSSA**	**I_2In**	**MBIn**
EN 12915-1	15	n.a.	n.a.	n.a.	n.a.	600	n.a.
BC1	42 (8)	10.5	253 (19)	81 (15)	53 (12)	129 (1)	4 (1)
BC2	12 (2)	8.6	243 (22)	43 (11)	63 (14)	144 (1)	4 (2)
BC3	14.1 (0.5)	8.4	153 (20)	65 (14)	76 (17)	88 (1)	1.4 (0.8)
BC4	29.2 (0.2)	9.1	222 (18)	92 (22)	117 (25)	124 (1)	4 (2)
BC5	49 (4)	12.0	302 (23)	121 (26)	97 (20)	156 (1)	6.0 (0.7)
BC6	25 (2)	11.0	309 (21)	80 (19)	136 (30)	197 (1)	4.1 (0.4)
BC7	6.2 (0.1)	7.0	136 (12)	33 (10)	40 (11)	77 (1)	2.2 (0.4)
AC1	7 (2)	10.9	1053 (88)	634 (118)	384 (81)	1010 (1)	20 (2)
AC2	13 (4)	9.9	714 (65)	300 (72)	359 (78)	540 (1)	15 (1)
AC3	21 (8)	8.1	561 (38)	205 (51)	273 (59)	438 (1)	11 (2)

Table 3 – Sorbent masses of chars (M, g) used in adsorption experiments of diiodoacetic acetic (DIAA), DIAA equilibrium concentrations (Ce, mg L^{-1}), DIAA removal (R, %), ratio of the amount of DIAA adsorbed per mass unit of sorbent (X/M, mg g^{-1}), and values of the Freundlich constant (K_F, $mg^{1-1/n}\ L^{1/n}\ g^{-1}$). Initial concentrations of DIAA tested for each char are reported in bracket.

M	Ce	R	X/M	K_F
BC6 (5 µg L^{-1})				
0.490	0.00146	70.8	0.00029	
0.324	0.00226	54.8	0.00034	
0.243	0.00272	45.6	0.00038	0.00484
0.163	0.00335	33.0	0.00040	
0.113	0.00377	24.6	0.00044	
0.084	0.00406	18.8	0.00045	
BC7 (5 µg L^{-1})				
0.459	0.00358	28.4	0.00012	
0.304	0.00402	19.6	0.00013	
0.218	0.00426	14.8	0.00014	0.00141
0.133	0.00454	9.2	0.00014	
0.103	0.00465	7.0	0.00014	
0.072	0.00475	5.1	0.00014	
AC1 (20 µg L^{-1})				
0.486	0.000032	99.8	0.00164	
0.323	0.000051	99.7	0.00247	
0.244	0.000102	99.5	0.00326	
0.163	0.000147	99.3	0.00487	3.18
0.122	0.000278	98.6	0.00647	
0.033	0.001510	92.5	0.02241	
0.017	0.001970	90.2	0.04242	
AC2 (20 µg L^{-1})				
0.244	0.000028	99.9	0.00327	
0.163	0.000048	99.8	0.00489	
0.122	0.000103	99.5	0.00652	0.922
0.083	0.000208	99.0	0.00954	
0.033	0.001630	91.9	0.02227	
0.016	0.002100	89.5	0.04475	

Table 4 – Mean values (n=3) and standard deviation (in bracket) of the removal performances (%) of 0.4 g of BC6, BC7, and AC1 towards 20 µg/L of DIAA, benzene, and 1,2-dichlororbenzene (contact time 24 h) in 100 mL-aliquots of two real water samples (DSB and CB) from a potabilization plant, in comparison with ultrapure water (UP). Tests were performed in triplicate. "Q" means quantitative removal, i.e. concentration of the contaminant at the end of the experiment below the detection limit.

	DIAA			**Benzene**			**1,2-Dichlorobenzene**		
	UP	**DSB**	**CB**	**UP**	**DSB**	**CB**	**UP**	**DSB**	**CB**
BC6	47 (1)	41 (3)	37 (2)	Q	Q	Q	Q	Q	Q
BC7	14 (2)	12 (3)	15 (3)	74 (10)	60 (12)	51 (9)	76 (9)	78 (11)	74 (10)
AC1	99 (1)	99 (4)	99 (3)	Q	Q	Q	Q	Q	Q

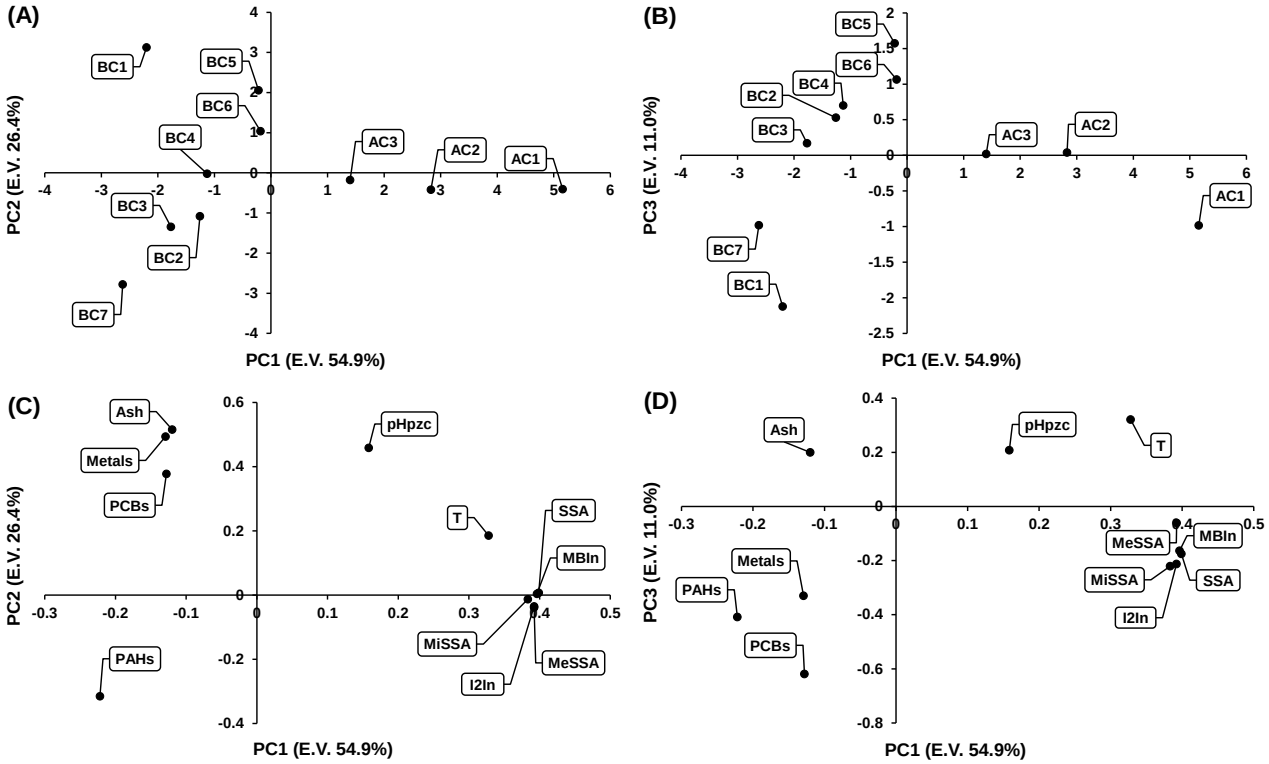

Figure 1 – Score (A-B) and loading (C-D) plots of PC1 versus PC2 and PC1 versus PC3, representing a percentage of explained variance (E.V.) of 81.3% and 65.9%, respectively. PCA values were calculated using the autoscaled values determined for the eleven original variables in the ten char samples. Note that the terms PAHs, PCBs, and Metals refer to their total leachable concentrations.

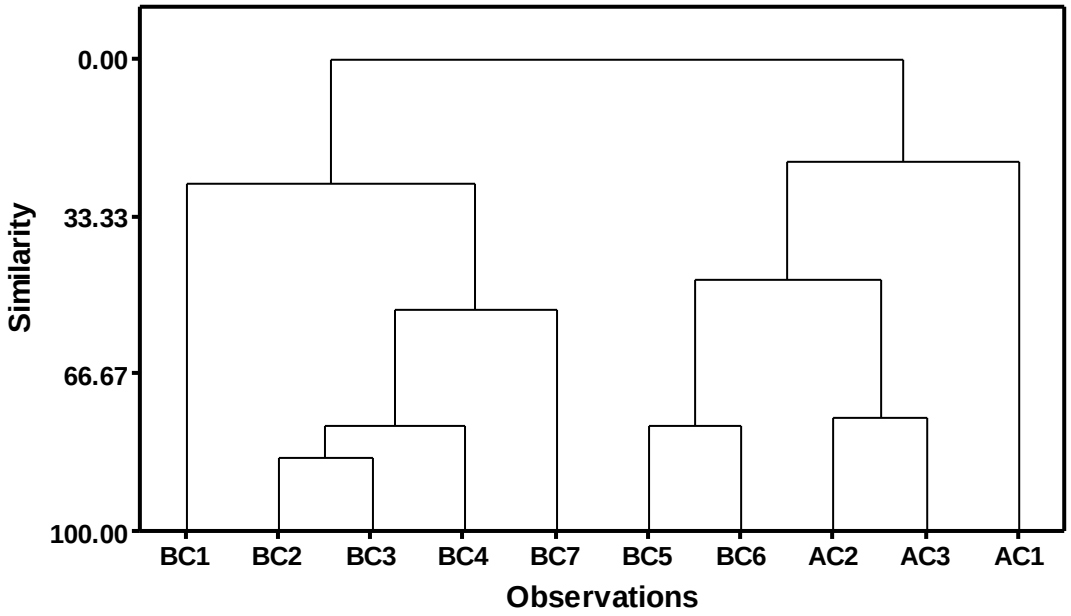

Figure 2 – Dendrogram of similarity of the ten investigated char samples, calculated through the complete linkage method on the basis of Euclidean distances of the autoscaled values of the eleven original variables.

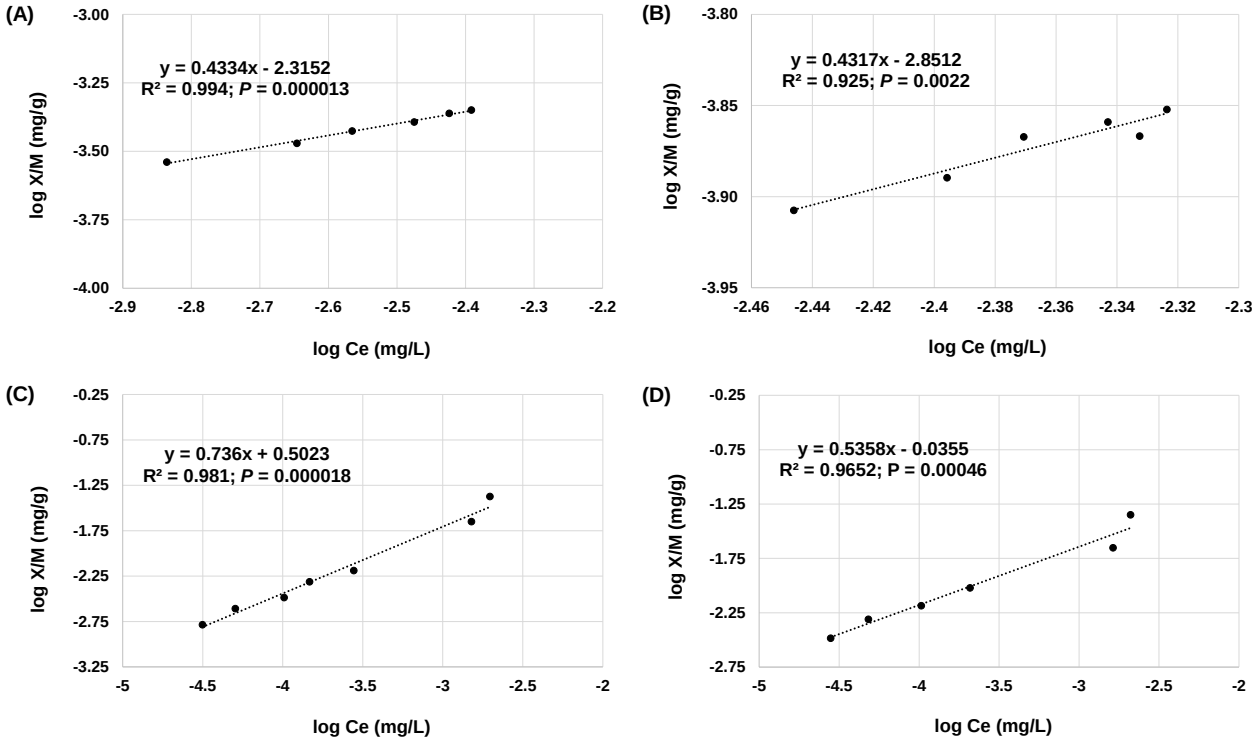

Figure 3 – Plots of linearized Freundlich isotherms obtained for BC6 (A), BC7 (B), AC1 (C), and AC2 (D).

SUPPLEMENTARY MATERIAL

Biochars intended for water filtration: a comparative study with activated carbons of their physicochemical properties and removal efficiency towards neutral and anionic organic pollutants

Michele Castiglioni[a], Luca Rivoira[a], Irene Ingrando[a], Lorenza Meucci[b], Rita Binetti[b], Martino Fungi[b], Ayoub El-Ghadraoui[c], Zaineb Bakari[c,d], Massimo Del Bubba[c], Maria Concetta Bruzzoniti[a*]

[a] Department of Chemistry, University of Turin, Via P. Giuria 5, 10125 Turin, Italy

[b] SMAT S.p.A., Research Centre, C.so Unità d'Italia 235/3, Turin, Italy

[c] Department of Chemistry "Ugo Schiff", University of Florence, Via della Lastruccia 3, 50019 Sesto Fiorentino, Italy

[d] National Engineering School of Sfax, Route de la Soukra km 4, 3038 Sfax, Tunisia

S1. Biochar and activated carbon characterization

The **physisorption analysis** of chars were performed by nitrogen adsorption and desorption experiments at -196°C using a Porosity Analyser Thermo Fisher (Milan, Italy) model SORPTOMATIC 1990. The surface area was calculated by using the Brunauer-Emmet-Teller (BET) and the Langmuir methods applied to nitrogen adsorption data in the relative pressure (P/P°) range of 0.05-0.25. The total pore volume was determined from the amount of nitrogen adsorbed at P/P°=0.98. The mesopore size distribution was determined by the Barret-Joyner-Halenda (BJH) model applied to desorption data and the assessment of microporosity was carried out by the t-plot method. For the porosimetry of biochars, a minimum equilibrium interval of 30 s with a maximum relative tolerance of 5% of the targeted pressure and an absolute tolerance of 5 mmHg were used. Before analysis, materials were degassed in situ, by heating at 300 °C, at a rate of 5 °C min^{-1}, under a high vacuum ($<10^{-8}$ mbar) for 12 h, provided by an oil sealed mechanical vacuum pump coupled with a high vacuum system. For the porosimetry a minimum equilibrium interval of 10 s with a maximum relative tolerance of 2% of the targeted pressure and an absolute tolerance of 2 mmHg were adopted.

The **ash content procedure** is provided by the ASTM International D 2866-11: a known amount of sorbent is placed in a muffle at 650 ° C for 1 hour and then weighted. According to the UNI EN 12902 standard, ashes should be below 15%.

The **pH at the zero-charge point (pH_{pzc})** was determined according to the pH drift method: 10 aliquots of 20 mL of 0.01 mol/L KNO_3 solution, whose pH was corrected in a range from 2 to 12, were prepared. 0.12 g of sorbent was added to each solution and, after stirring for 24 hours, the pH value was measured. To calculate the pH_{pzc}, the initial pH value of each solution was plotted against the final pH value: the pH_{pzc} corresponds to the intersection of the curve so obtained with the x axis.

The **extractable substances,** i.e. metals, Polycyclic Aromatic Hydrocarbons (PAHs) and Polychlorinated Biphenyls (PCBs), were determined for each sorbent following the UNI EN 12902 standard: 1 L of a solution containing $NaHCO_3$ (0.5 mmol/L), $CaCl_2$ (0.3 mmol/L), and $MgSO_4$ (0.2 mmol/L), at pH 7, was put in contact for 24 hours with 10 g of substrate. The content of Sb, As, Cd, Cr, Pb, Hg, Ni and Se was measured by ICP-MS, whereas PAHs and PCBs were determined by GC-MS. The analysis of a blank solution, without any material, was simultaneously performed.

For metals, a calibration curve was built from 0.25 to 20 µg/L; all the samples were acidified by 2% (v/v) HNO_3 before the ICP-MS analysis.

For the determination of PAHs and PCBs, the extracted solution was spiked with 23 ppt of labelled PAHs and PCBs (for apparent recovery calculation) and then pre-concentrated by solid phase extraction (SPE), using reversed phase cartridges according to *Environmental Engineering and Management Journal, 18(10), 2019, Pages 2133-2143*, and then analyzed by GC-MS.

The following operating conditions were adopted for GC-MS analysis. Column: HP 5MS UI (5% -phenyl)-methylpolysiloxane; Gas Carrier: He (1 mL/ min); Injection type: Pulsed Splitless; Injection pressure: 40 psi for 2.5 minutes: Injection volume 2 µl. The oven ramp was set as follows: starting temperature: 40°C, hold for 2 min; ramp to 176 °C, 12 °C/min rate; ramp to 196°C, 5 °C/min rate, hold for 3 mins; ramp to 224°C, 12 °C/min rate; ramp to 244 °C, 12°C/min rate, hold for 3 min; ramp to 270 °C, 7°C/min rate, hold for 3 min; final ramp to 300 °C, 5°C/min, hold for 10 min to completely clean and restore the GC column. The total run time for the complete separation of PAHs and PCBs is 52 min.

The **iodine index** was determined according to CEFIC test method. In detail, an aliquot of substrate (previously dried at 150 ° C until a constant mass is obtained) was boiled for 30 seconds in a flask with 10 mL of 5% HCl. Subsequently, 100 mL of a standardized 0.1N iodine solution (titrated by 0.1 N sodium thiosulfate) were added and the flask was shaken vigorously for about 30 seconds. The solution was immediately filtered on a gravity paper filter (first 20 mL aliquot is discarded).

Aliquots of 50 mL of the filtered solution were titrated with 0.10 M sodium thiosulfate until the yellow color disappeared after addition of 2 mL of a starch solution titration was continued until the blue color disappeared. The final volume of the sodium thiosulphate solution used was noted to evaluate the mg of iodine adsorbed.

The iodine number was calculated using the following formula:

$$I_n = \frac{X}{M} A$$

- $X = mg\ of\ iodine\ adsorbed\ by\ the\ material$
    - X = (12693 N_1) – (279.246 N_2 V) where N_1: normality of iodine solution, N_2: normality of thiosulphate solution; V is the volume of sodium thiosulphate solution in mL.
- M is the mass of activated carbon in g;
- A is the correction factor depending on the residual normality (Nr) of the filtrate and that is reported in a conversion table of CEFIC test method. This factor A may be applied if Nr is between 0.008 and 0.0334, when Nr = N_2 (V/50). If Nr is outside the range, the determination must be repeated.

The methylene blue index was determined according to CEFIC test method and represents the volume (mL) of a methylene blue solution (1.2 g/L) adsorbed by 0.1 g of sorbent placed in contact with it.

A methylene blue reference solution (C=1.2 g/L) was prepared, and its absorbance was measured diluting 5 mL of this solution with 0.25% (v/v) acetic acid to 1L. Absorbance measured at 620 nm should be 0.840±0.01; if higher, the reference solution should be diluted with ultrapure water to obtain the expected value.

Subsequently, 100 mg of dried sorbent were added to 25 mL of the 1.2g/L reference solution. The suspension is stirred for 30 minutes, filtered on a paper filter, discarding the first 5 mL of the filtrate and 1 mL of the filtered solution was diluted 1:100 in 0.25% acetic acid solution. Simultaneously, the reference solution was diluted 1:100 in 0.25% acetic acid. The absorbance of both solutions was measured at 620 nm.

The methylene blue index (x) is calculated according to:

$$x = \frac{ABSO\ x\ 25}{abs1}\ ;$$

- ABSO is the absorbance of methylene blue adsorbed by the sample, calculated as abs1 – abs2;
- abs 1 is the absorbance of the reference solution, diluted 1:100;
- abs 2 is the absorbance of the filtrate, diluted 1:100;

S2. Adsorption isotherms: determination of the residual concentrations of diiodoacetic acid by IC-MS/MS

Diiodoacetic acid was determined by IC-MS/MS using a Thermo Fisher Scientific (Waltham, MA USA) ICS-5000 IC system. The system includes a DP dual pump module for analytical and capillary applications, a CD conductivity detector, an AS autosampler, and a Reagent-Free (RFIC) eluent generator EG-5000 with ECG III cartridges KOH to provide the gradient of KOH (mobile phase) using deionized water from an AXP-MS pump (Thermo Fisher Scientific). For sample injections (120 µL), two autosamplers without (AS-DV) and with sample tray temperature control (AS-AP) set at 9±1 °C were used; both were from Thermo Fisher Scientific. Separations were performed on an IonPac AS24 (250x2 mm i.d.) coupled with a guard column IonPac AG24 (50x2 mm i.d.) both from Thermo Fisher Scientific, thermostatted at 15 °C in order to minimize the analyte degradation at high pH values. Eluent gradient (0.3 mL/min) was set as follows, 7 mM KOH: t=0-15.1 min; 7-15.5 mM KOH: t=15.1-25.8 min; 60 mM KOH: t=25.9 min, keep until 46 min; 7 mM KOH; t=47-58 min.

To remove trace anion contaminants from hydroxide eluent and to minimize base line shifts during gradient operation, an electrolytically continuously regenerated trap column (CR-ATC, 8% DVB crosslinking, 55 µm particle size) was installed in the eluent line after the pump prior to the sample injection. After eluent generation and before the separation column. Electrolytic suppression was accomplished using an ASRS 500 (2-mm) from Thermo Fisher Scientific.

A TSQ Endura triple-stage quadrupole mass spectrometer with ESI interface (HESI-II) was employed for detection. A diverter valve was used to waste the anion interfering species from matrix, thus preventing inorganic anions to enter the MS equipment. After the IC suppressor and before the ESI inlet, acetonitrile (CH_3CN) was added to the eluate at 0.3 mL/min through an additional AXP-MS pump. The m/z ratios of the precursor ion were 184.878 and 126.889, respectively. RF lens value was 51.236 V with CE 10.253 V.

S3. Adsorption isotherms: determination of the residual concentrations of VOCs by SPE-GC/MS

Benzene and 1,2-dichlorobenzene were extracted by solid-phase extraction (SPE) using a SPE Vacuum manifold and a polymeric reversed-phase cartridge (STRATA XL-100 µm, Phenomenex, Torrance, USA). The cartridge was firstly conditioned (20 psi) with 5 mL CH_2Cl_2, 5 mL 2-propanol, 5 mL H_2O, and then loaded (50 psi) with 100 ml of water sample. The water sample container was subsequently rinsed with 20 mL of a 2-propanol-water (10:90, v/v) solution. After loading, the cartridge was washed (20 psi) with 5 ml H_2O, and 5 mL of a 2-propanol-water (85:15, v/v) solution. The cartridge was dried for 10 min, capped, and analytes were finally eluted with two aliquots of 1.0 mL CH_2Cl_2. The eluted extract was finally diluted 50 times and injected for GC/MS analysis.

The following operating conditions were adopted for GC-MS analysis. Column: HP 5MS UI (5% -phenyl)-methylpolysiloxane; gas carrier: He (1.5 mL/ min); Injection type: Pulsed Splitless; Injection pressure: 40 psi for 2.5 minutes: Injection volume 2 µl.

The oven ramp was set as follows: starting temperature: 35°C, hold for 2 min; ramp to 50 °C, 4 °C/min rate; ramp to 120°C, 10 °C/min rate; ramp to 220°C, 30 °C/min rate, hold for 3 min. Retention times were 2.8 min for benzene and 10.8 min for 1,2-dichlorobenzene. Quantitative analysis were performed in SIM mode at the following m/z values: 78 (benzene) and 146 (1,2-dichlorobenzene).

Table S1 – Apparent recoveries of the SPE procedure for labelled PAHs and PCBs from the seven samples of biochars.

	BC 1	**BC 2**	**BC 3**	**BC 4**	**BC 5**	**BC 6**	**BC 7**
$^{13}C_6$-BaA	91.2 (0.1)	85.7 (1.6)	23.8 (4.3)	76.7 (3.6)	46.7 (2.1)	51.0 (3.8)	13.7 (1.1)
$^{13}C_6$-Chr	95.3 (0.5)	89.7 (1.1)	46.4 (2.9)	83.7 (7.0)	76.8 (1.4)	81.1 (2.2)	20.5 (2.2)
$^{13}C_6$-BbFl	76.0 (0.4)	83.3 (0.2)	19.4 (5.8)	73.5 (7.1)	61.2 (3.1)	76.4 (4.1)	15.4 (3.2)
$^{13}C_6$-BkFl	83.0 (3.5)	82.9 (2.1)	31.6 (1.9)	73.5 (4.3)	60.1 (2.5)	77.0 (3.6)	23.8 (3.3)
$^{13}C_4$-BaP	67.9 (4.3)	72.6 (1.5)	24.8 (7.3)	63.0 (4.5)	58.6 (3.0)	68.3 (2.8)	16.2 (0.4)
$^{13}C_4$-Ind	68.7 (6.8)	65.5 (1.6)	12.4 (3.1)	27.9 (0.1)	33.1 (2.6)	51.4 (3.1)	12.8 (1.1)
$^{13}C_6$-DBA	53.2 (2.1)	49.0 (1.3)	11.9 (2.4)	23.2 (1.7)	33.5 (2.9)	46.8 (1.1)	14.8 (4.3)
$^{13}C_{12}$-BP	57.8 (3.5)	48.5 (1.2)	14.7 (2.4)	27.4 (1.4)	36.7 (2.7)	45.8 (2.0)	14.2 (4.0)
$^{13}C_{12}$-PCB28	93.6 (2.8)	96.6 (4.0)	55.0 (9.5)	89.1 (3.8)	77.3 (3.1)	83.1 (4.1)	33.2 (4.5)

$^{13}C_{12}$-PCB52	90.6 (4.7)	97.3 (2.2)	60.6 (10.9)	92.4 (2.7)	70.8 (1.8)	76.7 (6.4)	37.7 (9.4)
$^{13}C_{12}$-PCB118	93.5 (0.7	76.2 (2.1)	32.8 (2.3)	58.5 (5.2)	55.2 (4.1)	61.0 (3.7)	11.5 (5.7)
$^{13}C_{12}$-PCB153	86.9 (1.4)	79.4 (3.1)	35.8 (1.1)	59.8 (6.8)	54.7 (2.5)	58.8 (2.0)	13.3 (6.4)
$^{13}C_{12}$-PCB180	71.0 (3.5)	75.2 (1.8)	24.5 (8.2)	52.0 (13.0)	48.1 (2.8)	61.0 (4.4)	9.0 (3.6)

Table S2 – Apparent recoveries of the SPE procedure for labelled PAHs and PCBs from the three samples of activated carbons.

	AC1	**AC2**	**AC3**
$^{13}C_6$-BaA	60.6 (14.4)	96.3 (5.0)	61.9 (14.6)
$^{13}C_6$-Chr	75.2 (20.6)	94.5 (6.4)	76.0 (20.6)
$^{13}C_6$-BbFl	49.8 (11.6)	51.4 (2.7)	55.1 (12.9)
$^{13}C_6$-BkFl	59.0 (13.3)	52.8 (2.1)	58.0 (13.6)
$^{13}C_4$-BaP	39.5 (9.2)	48.3 (2.2)	48.2 (11.3)
$^{13}C_4$-Ind	13.8 (2.5)	47.3 (0.2)	16.8 (3.7)
$^{13}C_6$-DBA	13.8 (2.0)	35.4 (3.2)	19.9 (4.6)
$^{13}C_{12}$-BP	12.7 (1.1)	34.4 (0.5)	18.9 (4.4)
$^{13}C_{12}$-PCB28	43.6 (6.4)	76.2 (1.0)	56.4 (12.5)
$^{13}C_{12}$-PCB52	30.5 (3.5)	72.7 (12.6)	55.0 (14.1)
$^{13}C_{12}$-PCB118	16.6 (3.3)	49.5 (12.4)	37.6 (11.2)
$^{13}C_{12}$-PCB153	13.7 (3.4)	55.2 (5.3)	28.2 (8.6)
$^{13}C_{12}$-PCB180	12.1 (2.7)	52.3 (5.9)	19.5 (5.5)

The evaluation of extracted PAHs and PCBs was preceded by the determination of SPE extraction recovery of labelled surrogates from each char. Apparent recoveries were calculated after spiking the extracted solutions with labelled surrogates and were expressed as average of two replicated SPE extractions on two spiked aliquots of char. Hence, averages are referred to n=14 and n= 6 data for the seven biochar, and for the three activated carbons, respectively.

For biochars, average recoveries were 50.7% for PAHs (relative standard deviation, RSD, below 7.0%) and 62.1% for PCBs (RSD below 7.0%). For activated carbons, average recoveries were 47.4% for PAHs (RSD below 21%) and 41.3% for PCBs (RSD below 13%).

It is interesting to note that for both PAHs and PCBs, the average of apparent extraction recoveries for ACs is lower than that observed for BCs. This may be ascribed to a higher matrix effect exhibited by ACs due to possible leaching from the material. This hypothesis is supported by the higher RSD values observed for ACs with respect to BCs and by the total organic carbon measurements (see *Adsorption tests in real water samples* section) performed on selected BC and AC samples.

Additionally, for both the classes of biochar and activated carbon, extraction recoveries increase with the decrease of log P of analytes (data not shown), in agreement with the lower competitive effect exhibited by the reversed-phase cartridge used during SPE experiments.

S4. Release of PAHs, PCBs, and metals from biochars and activated carbons

Table S3 – Extractable PAHs from the chars studied. Concentrations are expressed in ng/L. The sum of concentrations of asterisked PAHs (regulated by the UNI EN 12915-1) is also reported. Regulated limit for these compounds is 20 ng/L.

	BC1	**BC2**	**BC3**	**BC4**	**BC5**	**BC6**	**BC7**	**AC1**	**AC2**	**AC3**
Naphthalene	0.55 (0.01)	< LOD	21.9 (0.97)	4.15 (0.07)	6.64 (20)	7.2 (0.13)	83.14 (3.69)	2.2 (0.09)	12.5 (0.45)	10.91 (0.24)
Acenaphthylene	< LOD	< LOD	0.99 (0.03)	1.18 (0.08)	0.56 (0.07)	0.94 (0.01	6.22 (0.18)	< LOD	< LOD	< LOD
Acenaphthene	0.9 (0.5)	< LOD	3.77 (0.06)	0.94 (0.09)	2.04 (0.09)	2.2 (0.53)	33.34 (3.17)	< LOD	2.73 (0.07)	3.03 (0.15)
Fluorene	< LOD	3.56 (0.41)	83.26 (3.42)	8.34 (0.2)	< LOD	< LOD	261.55 (13.33)	1.04 (0.03)	2.34 (0.11)	3.29 (0.21)
Phenantrene	15 (4)	34.47 (0.75)	164.25 (5.56)	8.00 (0.03)	< LOD	< LOD	329.54 (19.31)	7.04 (0.03)	4.92 (0.21)	7.52 (0.15)
Anthracene	1.7 (0.01)	4.36 (0.06)	36.77 (0.94)	0.88 (0.07)	< LOD	< LOD	72.03 (2.84)	1.99 (0.17)	2.02 (0.28)	2.69 (0.03)
Fluoranthene*	3.37 (0.01)	7.21 (0.07)	3.41 (0.20)	1.64 (0.03)	< LOD	< LOD	12.71 (0.3)	< LOD	< LOD	< LOD
Pyrene	3.09 (0.48)	6.36 (0.14)	5.56 (0.03)	0.98 (0.01)	2.05 (0.15)	1.45 (0.07)	26.64 (0.8)	< LOD	0.87 (0.06)	1.11 (0.07)
Benzo[a]pyrene	< LOD	< LOD	< LOD	< LOD	< LOD	< LOD	< LOD	< LOD	< LOD	< LOD
Chrysene	0.96 (0.14)	< LOD	1.34 (0.09)	< LOD	< LOD	< LOD	< LOD	< LOD	< LOD	< LOD
Benzo[b]fluoranthene*	1.95 (0.42)	< LOD	< LOD	< LOD	< LOD	< LOD	< LOD	< LOD	< LOD	< LOD
Benzo[k]fluoranthene*	1.53 (0.30)	< LOD	< LOD	< LOD	< LOD	< LOD	0.55 (0.11)	< LOD	< LOD	< LOD
Benzo[g,h,i,]perylene*	< LOD	< LOD	< LOD	< LOD	< LOD	< LOD	< LOD	< LOD	< LOD	< LOD
Indeno[1,2,3-c,d]pyrene*	< LOD	< LOD	< LOD	< LOD	< LOD	< LOD	< LOD	< LOD	< LOD	< LOD
Dibenzo[a,h]anthracene	< LOD	< LOD	< LOD	< LOD	< LOD	< LOD	< LOD	< LOD	< LOD	< LOD
Benzo[g,h,i,]perylene*	< LOD	< LOD	< LOD	< LOD	< LOD	< LOD	< LOD	< LOD	< LOD	< LOD
Σ* UNI EN 12915-1	6.85	7.21	3.41	1.64	< LOD	< LOD	13.26	< LOD	< LOD	< LOD
Σ	29.39	55.96	321.25	26.11	11.29	11.79	825.72	12.27	25.38	28.55
Σ (Benzo[a]pyrene eq. conc.)	0.398	0.095	0.664	0.034	0.011	0.012	1.528	0.030	0.044	0.053

Table S4 – Extractable PCBs from the chars studied. Concentrations are expressed in ng/L.

	BC1	BC2	BC3	BC4	BC5	BC6	BC7	AC1	AC2	AC3
PCB15	0.5 (0.1)	0.56 (0.05)	1.29 (0.02)	2.8 (0.1)	21.7 (0.1)	29 (1)	20 (2)	< LOD	4 (2)	1.1 (0.2)
PCB101	6.3 (0.2)	< LOD	< LOD	< LOD	< LOD	< LOD	< LOD	< LOD	< LOD	< LOD
PCB81	8 (2)	< LOD	< LOD	< LOD	< LOD	< LOD	< LOD	< LOD	< LOD	< LOD
PCB118	7 (2)	< LOD	< LOD	< LOD	< LOD	< LOD	< LOD	< LOD	< LOD	< LOD
PCB123	12 (3)	< LOD	< LOD	< LOD	< LOD	< LOD	< LOD	< LOD	< LOD	< LOD
PCB153	16 (4)	< LOD	< LOD	< LOD	< LOD	< LOD	< LOD	< LOD	< LOD	< LOD
PCB167	21 (5)	< LOD	< LOD	< LOD	< LOD	< LOD	< LOD	< LOD	< LOD	< LOD
PCB180	25 (7)	< LOD	< LOD	< LOD	< LOD	< LOD	< LOD	< LOD	< LOD	< LOD
Σ	95.8	0.56	1.29	2.8	21.7	29	20	< LOD	4	1.1

Table S5 – Extractable metals from the chars studied. Concentrations are expressed in µg/L. The limits established by the UNI EN 12915-1 are also reported.

	BC1	BC2	BC3	BC4	BC5	BC6	BC7	AC1	AC2	AC3	UNI EN limits
Cd	< LOD	< LOD	< LOD	< LOD	< LOD	< LOD	< LOD	< LOD	< LOD	< LOD	0.5
As	< LOD	< LOD	< LOD	< LOD	< LOD	< LOD	< LOD	< LOD	< LOD	< LOD	10
Cr	**17.3 (0.1)**	< LOD	< LOD	2.8 (0.1)	3.1 (0.1)	3.45 (0.07)	< LOD	< LOD	< LOD	< LOD	5
Ni	< LOD	< LOD	< LOD	< LOD	< LOD	< LOD	< LOD	< LOD	< LOD	< LOD	15
Pb	< LOD	< LOD	< LOD	< LOD	< LOD	< LOD	< LOD	< LOD	< LOD	< LOD	5
Sb	< LOD	< LOD	0.73 (0.05)	< LOD	1.07 (0.01)	2.68 (0.05)	< LOD	< LOD	< LOD	< LOD	3
Se	< LOD	< LOD	< LOD	< LOD	1.01 (0.02)	0.55 (0.08)	< LOD	< LOD	< LOD	**5.0 (0.2)**	3
Hg	< LOD	< LOD	< LOD	< LOD	< LOD	< LOD	< LOD	< LOD	< LOD	< LOD	0.3

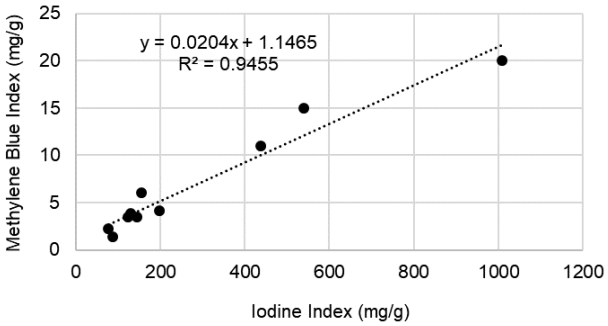

Figure S1 – Dispersion plot and least square regression line of I_2In vs. MBIn.

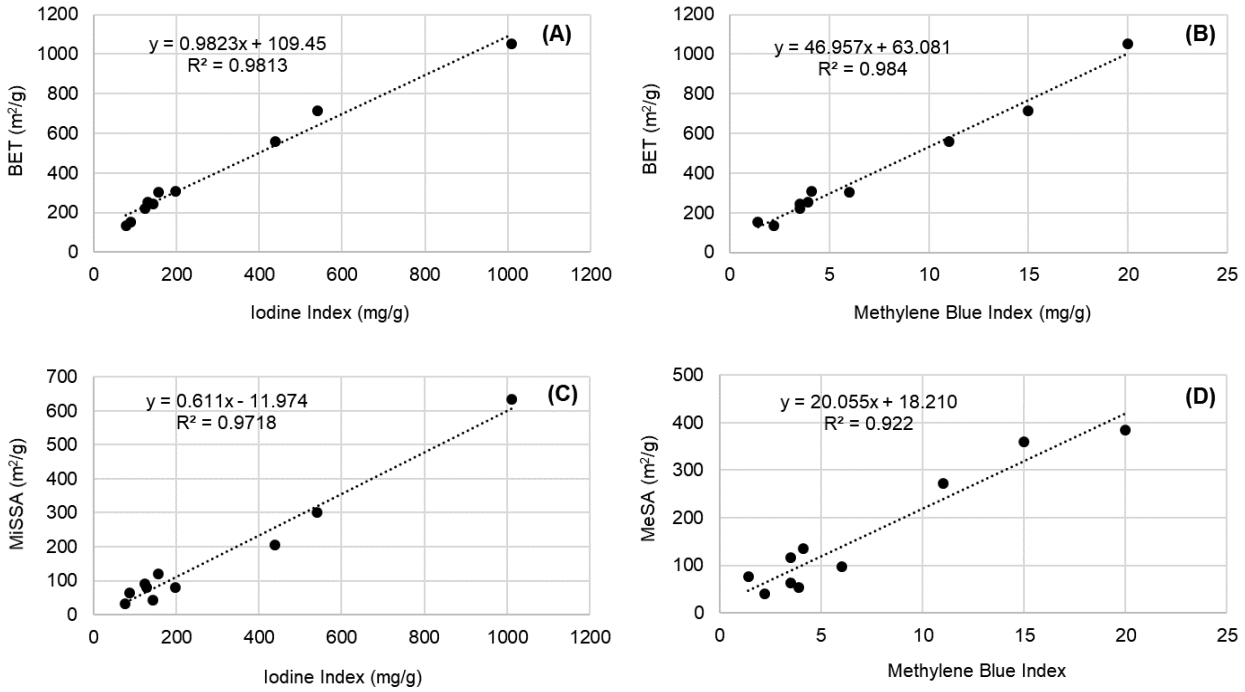

Figure S2 – Dispersion plots and least square regression lines of (A) BET specific surface area vs. I_2In, (B) BET specific surface area vs. MBIn, (C) micropore specific surface area vs. I2In, and (D) mesopore specific surface area vs. MBIn.